Published in final edited form as:
Langmuir. 2012 October 9; 28(40): 14273–14283. doi:10.1021/la3029935.

Non-Fouling Poly(ethylene oxide) Layers End-Tethered to Polydopamine

Ognen Pop-Georgievski[†], **Dominique Verreault**[‡,¶,||], **Mark-Oliver Diesner**[¶], **Vladimír Proks**[†], **Stefan Heissler**[§], **František Rypácek**[†], and **Patrick Koelsch**[*,‡,¶,⊥]
Institute of Macromolecular Chemistry, Academy of Sciences of the Czech Republic, Heyrovsky Square 2, 162 06 Prague 6, Czech Republic, Department of Applied Physical Chemistry, University of Heidelberg, Im Neuenheimer Feld 253, D-69120 Heidelberg, Germany, Institute of Toxicology and Genetics, Karlsruhe Institute of Technology (KIT), Hermann-von-Helmholtz-Platz 1, D-76344 Eggenstein-Leopoldshafen, Germany, and Institute of Functional Interfaces, Karlsruhe Institute of Technology (KIT), Hermann-von-Helmholtz-Platz 1, D-76344 Eggenstein-Leopoldshafen, Germany

Non-fouling surfaces capable of reducing protein adsorption are highly desirable in a wide range of applications. Coating of surfaces with poly(ethylene oxide) (PEO), a water-soluble, non-toxic, and non-immunogenic polymer, is most frequently used to reduce non-specific protein adsorption. Here we show how to prepare dense PEO brushes on virtually any substrate by tethering PEO to polydopamine (PDA)-modified surfaces. The chain lengths of hetero-bifunctional PEOs were varied in the range of 45 to 500 oxyethylene units (M_n = 2000–20000). End-tethering of PEO chains was performed through amine and thiol headgroups from reactive polymer melts to minimize excluded volume effects. Surface plasmon resonance (SPR) was applied to investigate the adsorption of model protein solutions and complex biologic medium (human blood plasma) to the densely packed PEO brushes. The level of protein adsorption of human serum albumin and fibrinogen solutions was below the detection limit of the SPR measurements for all PEO chains end-tethered to PDA, thus exceeding the protein resistance of PEO layers tethered directly on gold. It was found that the surface resistance to adsorption of lysozyme and human blood plasma increased with increasing length and brush character of the PEO chains end-tethered to PDA with a similar or better resistance in comparison to PEO layers on gold. Furthermore, the chain density, thickness, swelling, and conformation of PEO layers were determined using spectroscopic ellipsometry (SE), dynamic water contact angle (DCA) measurements, infrared reflection-absorption spectroscopy (IRRAS), and vibrational sum-frequency-generation (VSFG) spectroscopy, the latter in air and water.

[*]To whom correspondence should be addressed: koelsch@uw.edu.
[†]Institute of Macromolecular Chemistry, Academy of Sciences of the Czech Republic
[‡]Department of Applied Physical Chemistry, University of Heidelberg
[¶]Institute of Toxicology and Genetics, Karlsruhe Institute of Technology
[§]Institute of Functional Interfaces, Karlsruhe Institute of Technology
[||]Current address: Department of Chemistry and Biochemistry, The Ohio State University, 100 West 18th Avenue, Columbus, OH 43210, USA
[⊥]Current address: National ESCA and Surface Analysis Center for Biomedical Problems, Department of Bioengineering, University of Washington, Box 35170, Seattle, WA 98195-1750, USA

Notes
The authors declare no competing financial interest.

Supporting Information
Hydrodynamic radius (R_h) determined by DLS and calculated radius of gyration (R_g) for the PEO's used in this study, chemical schemes of PDA covalent structure, calculations of the interpenetration zone thickness, ellipsometric data on PEO layer thickness and surface chain density, explanation for the VSFG delay shifting procedure, normalized and delay-shifted VSFG spectra of PDA and PEO layers in the C–H region. This material is available free of charge at http://pubs.acs.org

INTRODUCTION

The suppression of non-specific protein adsorption at the solid-liquid interface is a crucial issue for biomedical and biotechnological applications.[1,2] For example, in many biosensing devices a specific response imparted by the presence of certain bioactive ligands on the material surface can be distinguished from non-specific adsorption only in the presence of a protein-resistant background.[2–4] Coating of the substrate surface with brushes of poly(ethylene oxide) (PEO), a water soluble, non-toxic, and non-immunogenic polymer, is among the most frequently used approaches to reduce non-specific protein adsorption.[5]

Several experimental studies have pointed out the importance of PEO brush parameters like chain density, brush thickness, molecular weight, and hydrophilicity with respect to the ability of PEO to suppress protein adsorption.[6–16] However, there is still a lack in understanding the conformation, organization, and behavior of the dense PEO brushes in water. Furthermore, most of the proposed approaches of PEO anchoring are substrate-specific and/or lead to low grafting densities.

Inspired by the composition of mussel adhesive proteins, Lee *et al.* proposed a method to form multifunctional polymer coatings by simple dip-coating of different materials in an aqueous solution of dopamine.[17] Under alkaline conditions, dopamine spontaneously oxidizes and forms highly reactive products such as 5,6-dihydroxyindole, 5,6-indole-semiquinone and -quinone. [17] These further react to form water insoluble oligomers or polymers through polycondensation between the indole units (Scheme 1A).[18] The oligomers self-assemble and form colloidal particles that further aggregate, resulting in a black precipitate in the solution and a thin layer on the surfaces in contact with the solution. The PDA film formation most probably proceeds by both polymerization from the surface and adsorption of the colloidal particles formed in the solution.[19] The final covalent structure of PDA remains elusive. While earlier studies depict PDA as a high molecular weight polymer made up of randomly linked monomer units,[20,21] more recent ones suggest ultrastructural organization of 4–5 π-stacked oligomeric sheets.[18,22] The strength of PDA binding to materials originates from the reactivity of orthoquinone/catechol subunits that can form coordination bonds with surface metal oxides and covalent bonds with nucleophilic groups. With the accompanying weaker interactions such as hydrogen bonds, van der Waals interactions, π– π stacking and hydrophobic interactions the PDA layer can strongly bind onto a wide range of inorganic and organic materials, including noble metals, oxides, polymers, semiconductors, and ceramics. Furthermore, it has been shown that the PDA chemical composition[17] and growth kinetics[19] are independent from the chemical structure of the substrate. The significant chemical diversity of PDA[17,18,20–22] can be used in a variety of reactions with organic species for the creation of functional organic ad-layers. Particularly, the unsaturated indole rings and the catechol groups of the different monomer units, via Michael addition and Schiff base formation, react with nucleophilic groups such as thiol-and amino-termini of PEO chains[17] to form densely packed PEO brushes (Scheme 1B).[19]

The PDA/PEO modification route represents a substrate-independent approach for protein-repellent layer formation on literally any solid substrate. Recently, on a similar basis Proks *et al.* proposed the “Click & Seed” modification approach for precise incorporation of biomimetic cell adhesion ligands on the PDA/PEO surface.[23]

In this work, end-tethered dense PEO brushes were prepared on PDA-modified and bare gold substrates. The chain lengths of hetero-bifunctional PEOs, α-aminoethyl-ω-methoxy-PEO and α-thiolethyl-ω-methoxy-PEO, were varied in the range of 45 to 500 oxyethylene units (M_n = 2000–20000). The end-tethering of PEO chains was performed from reactive

polymer melt in order to minimize excluded volume effects, a crucial factor in controlling the upper limit of grafting density.[24–26] The obtained PEO layers were characterized by spectroscopic ellipsometry (SE) and water dynamic contact angle (DCA) measurements. In order to study protein-repellent properties of surfaces, adsorption of single protein solutions like human serum albumin,[27] fibrinogen,[6,7,28,29] lysozyme,[6,7] and to a lesser extent complex biological media like blood plasma[30] have been performed. Here, surface plasmon resonance (SPR) was applied to study the adsorption from model (fibrinogen, albumin, lysozyme) and complex (human blood plasma) protein solutions to these surfaces. Finally, *ex situ* infrared reflection-absorption spectroscopy (IRRAS) and *ex situ* and *in situ* vibrational sum-frequency-generation (VSFG) spectroscopy experiments were performed to examine differences in conformation of the polymer layers in air and water.

MATERIALS AND METHODS

Materials

Dopamine hydrochloride (98.5%), human serum albumin (HSA), fibrinogen (Fbg), and lysozyme (Lys) were purchased from Sigma-Aldrich (Germany). Citrated and mixed human blood plasma (HBP) from five healthy donors was obtained from the Institute of Hematology and Blood Transfusion (Prague, Czech Republic). Hetero-bifunctional PEOs, α-aminoethyl-ω-methoxy-PEO and α-thiolethyl-ω-methoxy-PEO, were used for the preparation of polymer brushes (Rapp Polymere, Germany). The number average molecular weights of the polymers were 2015, 5118, 11153, 22271 g/mol for the thiol-PEO's and 1930, 5079, 11065, 22359 g/mol amino-PEO's. The index of polydispersity for all polymers was 1.03. Although throughout the text we use the nominal values of 2000, 5000, 10000, and 20000 g/mol, all calculations were performed using the previously stated M_n's. Organic solvents of analytical grade were used as received.

Substrate Preparation

One-side polished Si wafers (CZ, orientation <100>, B-doped, resistivity 5–22 Ω·cm) were coated with a 2.5 nm Ti adhesion layer and, subsequently, with a 200 nm-thick Au layer using RF magnetron sputtering. Wafers were cut into 1.2 cm×2.4 cm pieces. Samples were sonicated in methanol and deionized water (MilliQ system, Millipore, USA) for 15 min, immersed in a mixture of 25% ammonia, 30% hydrogen peroxide and water (1:1:5, (v/v/v)) heated at 70 °C for 10 min, and finally thoroughly rinsed with water and ethanol. Dry samples were cleaned by UV-ozonolysis (UVO Cleaner, Jelight, USA) for 2 h prior to PEO or PDA deposition. Gold-coated substrates for SPR analysis were purchased from Litcon (Sweden) and consisted of N-BK7 glass supports coated with a ~2 nm-thick Ti adhesion layer and a ~50 nm-thick Au layer. These were treated in the same manner as the gold samples prepared on Si substrates.

Preparation of PDA

PDA was deposited from 2 mg/mL solution prepared by dissolution of dopamine hydrochloride in 10 mM Tris-HCl buffer at pH 8.5 (Scheme 1A). The deposition on substrates was performed in open glass dishes under stirring to provide a continuous supply of oxygen through the air/solution interface. In addition, the substrates were kept vertical to suppress microparticle sedimentation. After 3 h of polymerization the PDA-coated surfaces were rinsed with water, sonicated in water for 15 min, and blown dry in a stream of purified nitrogen, to obtain a 12 nm-thick PDA anchor layer.

PEO Grafting

α-Aminoethyl-ω-methoxy-PEO and α-thiolethyl-ω-methoxy-PEO were applied from melt to substrates with a PDA anchor layer (Scheme 1B). In parallel, reference grafting through thiolate formation between the α-thiolethyl-ω-methoxy-PEO and the bare gold substrates was performed from melt. This reaction facilitates the high affinity of thiols to gold (Scheme 1C). The molecular weight of the polymers was varied from 2000 to 20000 g/mol (containing from 45 to 500 ethylene oxide (EO) units). The grafting was performed at 110 °C in vacuum from a several micron-thick layer formed by drying of 8 mg/mL solution amino-PEO and thiol-PEO in methanol at a surface coverage of 2 μg/mm^2. After 8 h of grafting, the substrates were rinsed with copious amounts of water, then immersed in water at 40 °C for 1 h under stirring to remove non-covalently bound fraction of PEO, and finally dried in vacuum.

Spectroscopic Ellipsometry

Ellipsometric data were acquired using a SENpro ellipsometer (SENTECH Instruments, Germany) in rotating analyzer mode at an angle of incidence (AOI) of 70° in the spectral range of 370–1050 nm. *In situ* ellipsometry data were acquired using a spectroscopic imaging auto-nulling ellipsometer (EP^3-SE, Nanofilm Technologies, Germany) equipped with a liquid cell (V = 0.7 mL) in 4-zone mode in the wavelength range of 398.9–811 nm (source: Xe arc lamp, wavelength step: 10 nm) at AOI = 60°. The cell windows (strain-free, optical BK-7 glass from Qioptiq, Germany) exhibited only small birefringence and/or dichroism causing errors in Δ and Ψ smaller than 0.3° and 0.1°, respectively. These errors were corrected following the method of Azzam and Bashara.[31] To increase the measurement precision and exclude errors from the variations of layer thickness throughout the substrate area, a 10× objective and position-calibrated sample stage were utilized to perform repeated *ex situ* and *in situ* measurements over the same sample area (1 mm × 2 mm). The obtained data were analyzed with SpectraRay LT and EP^3 softwares. The optical constants of PDA in air were taken from a previous study,[19] while those of the swollen PDA were determined utilizing the interference enhancement method on 250 nm-thick SiO_2/Si substrates.[32]Polymer thickness and complex refractive index were obtained from simultaneous fitting using Cauchy dispersion functions ($n = A_n + B_n/\lambda^2$ and $k = A_k + B_k/\lambda^2$ with A_n = 1.450 ± 0.091, B_n = 5900 ± 150 [nm^2], k = 0 for PEO in air; A_n = 1.376 ± 0.004, B_n = 3711 ± 831 [nm^2], k = 0 for swollen PEO; A_n = 1.642 ± 0.038, B_n = −28597 ± 358 [nm^2], A_k = 0.019 ± 0.002, B_k = 26781 ± 5100 [nm^2] for swollen PDA). The dispersion function of the bare gold layer was obtained by fitting the parameters of one Drude-Lorentz and two Lorentz oscillators. Note that gold layers thicker than ~40 nm are practically non-transparent in the used range of wavelengths. The optical constants of the SiO_2/Si substrates were taken from elsewhere.[33]

Dynamic Light Scattering (DLS)

DLS measurements were carried out on an ALV instrument (ALV-Laser Vertriebsgesellschaft, Germany) in the angular range 30–140°. An ALV 5000, multibit, multitau autocorrelator covering approximately 12 decades in the delay time τ was used for measurements of time autocorrelation functions. The obtained scattered light intensity distribution function $A(\tau)$ can be easily transformed into a distribution function of hydrodynamic sizes. [34] The hydrodynamic radius R_h was calculated from the diffusion coefficient D, using the Stokes-Einstein equation: $R_h = \frac{k_B T}{6\pi\eta D}$, where k_B is the Boltzmann constant, T is the absolute temperature and η (0.894 mPa·s) is the dynamic viscosity of water at 25 °C.[35] The experimental error of R_h determination was typically about 3%. Assuming that the PEO chains in good solvent are randomly coiled, the radius of gyration

R_g can be calculated as: $R_g = 1.78 \times R_h$.[36] The obtained results are summarized in Table S1 in the Supporting information.

Calculations of Grafting Density, Distance Between Grafting Sites, Structural State and Degree of Swelling of PEO Chains in Water

The PEO thicknesses obtained from the ellipsometry measurements were used to calculate the grafting density $\sigma = h\rho N_A/M_n$ and distance between grafting sites $D = (4/\pi\sigma)^{1/2}$, where h is the layer thickness in the dry state as determined by ellipsometry,[24,25,37] $\rho = 1.09$ g/cm^3 is the PEO bulk density, and N_A is the Avogadro constant. The ratio of the distance between PEO chains to R_g describes the overlap of the tethered chains. The overlap parameter ($D/2R_g$) can be used to determine the structural state of the bound chains: [15] (i) for $D/2R_g > 1$, the polymer chains are in a "mushroom" state, i.e., reside isolated on the surface with only little interaction with neighboring polymer chains; (ii) values of $D/2R_g = 1$ are characteristic for the "mushroom-to-brush transition" where neighboring chains begin to overlap and interact with one another; (iii) for $D/2R_g < 0.5$, the polymer chains are in a "brush" state where there is significant chain overlap between the neighboring chains, forcing them to extend away from the surface. The ratio of the layer thickness in water h_{H_2O} measured by *in situ* SE to the thickness in dry state gives the percentage of swelling in water according to $p_{H_2O} = (h_{H_2O}/h) \times 100\%$.

Infrared Reflection-Absorption Spectroscopy

The infrared spectra of the layers were recorded using a VERTEX 80 FT-IR spectrometer (Bruker Optics, Germany) equipped with a grazing angle (85°) reflection spectroscopy accessory. The measurement chamber was continuously purged with dry air. The acquisition time was around 20 min at a resolution of 2 cm^{-1}. The spectra are reported as $-\log(R/R_0)$, where R is the reflectance of the sample and R_0 is the reflectance of a deuterated hexadecanethiol ($HS(CD_2)_{15}CD_3$) self-assembled monolayer (SAM) on gold.

Vibrational Sum-Frequency-Generation Spectroscopy

VSFG spectra were recorded using a partially custom-built broadband SFG spectrometer described elsewhere.[38] The setup utilizes ~100 fs infrared pulses at an energy of 4 μJ/pulse with a repetition rate of 1 kHz. These are overlapped spatially and temporally at the sample surface with etalon-shaped, narrowband visible pulses at 800 nm wavelength. The resulting VSFG signal is dispersed by a monochromator and subsequently imaged by a backlight-illuminated CCD camera. All spectra were recorded in *ppp* polarization (i.e. sum-frequency (SF), visible (VIS), and infrared (IR) *p*-polarized beams) at incidence angles of 60° and 70° for the VIS and IR beams, respectively. Each sample was measured in air and in water using the thin-layer analysis (TLA) cell previously described.[38] Samples were probed through a half-cylindrical CaF_2 prism and a thin layer of water located above the sample. Every sample was kept in the cell filled with water for 10 min prior to measurement. Spectral acquisition time was 10 s for each spectrum and all spectral positions were calibrated using a do-decanethiol (DDT) SAM on gold. VSFG spectra of films on gold substrates show an intense non-resonant signal originating from electronic interband transitions within the metal together with a resonant signal emanating from the film of interest. The relative phase between non-resonant and resonant signals determine the shape of the bands. For example, the presence of peaks or dips in the non-resonant signal can be related to relative phases around 0 or π, respectively. These values have been shown to depend on the orientation of the probed chemical group (e.g., CH-containing groups). Hence, having a chemical group with its transition dipole moment (TDM) oriented towards or away from the substrate leads to a constructive (peak) or a destructive (dip) interference, respectively.[39,40]

The intensity of the generated SF signal at a given IR frequency ω is related to the infrared (I_{IR}) and visible (I_{VIS}) input intensities by the relation:

$$\begin{aligned} I_{SF}(\omega) &\propto \left|\chi^{(2)}\right|^2 I_{IR} I_{VIS}, \\ &\propto \left|\chi^{(2)}_{NR} + \chi^{(2)}_{R}(\omega)\right|^2 I_{IR} I_{VIS}, \\ &\propto \left|\left|\chi^{(2)}_{NR}\right| \exp(i\varphi_{NR}) + \left|\chi^{(2)}_{R}(\omega)\right| \exp(i\varphi_{R}(\omega))\right|^2 I_{IR} I_{VIS}, \end{aligned} \quad (1)$$

where $\chi^{(2)}_{NR}$ and $\chi^{(2)}_{R}$ are the non-resonant and resonant contributions, respectively, to the second-order nonlinear susceptibility.

Surface Plasmon Resonance

Protein adsorption was measured with a custom-built SPR instrument (Institute of Photonics and Electronics, Academy of Sciences of the Czech Republic) utilizing the Kretschmann geometry to excite surface plasmons.[3] The SPR chips were coated with 12 ±0.8 nm PDA layer onto which PEO layers were subsequently grafted. HSA (5 mg/mL), Fbg (1 mg/mL), Lys (1 mg/mL), and 100% HBP in PBS (pH 7.4) were injected as analytes through the flow cell at a rate of 20 μL/min for 20 min. Protein-surface interactions were monitored in real-time as shifts in the resonant wavelength $\Delta\lambda_{res}$ (wavelength interrogation detection mode at constant AOI = 60°). The $\Delta\lambda_{res}$ between two buffer baselines obtained before and after protein injection was used to calculate the amount of irreversibly bound proteins to the surface. The observed $\Delta\lambda_{res}$ reflects the changes in the refractive index of the medium at the sensor surface within the penetration depth of the SPR evanescent wave as a result of (i) changes in mass deposited at the sensor surface and (ii) of the exchange of solutions of different refractive indexes proportional to different protein and salt concentrations. For the SPR sensor used in this study, a shift in $\Delta\lambda_{res}$ of 1 nm corresponds to a surface coverage of 15 ng/cm^2. The latter value was estimated by comparing the IRRAS spectrum of a known amount of HSA deposited on an SPR chip and has been readily reported in the literature.[41,42] The detection limit of the SPR instrument was estimated to be the sensor response corresponding to three standard deviations of the baseline noise. The average detection limit was 0.045 nm which corresponds to 0.7 ng/cm^2.

Dynamic Contact Angle Measurement

The dynamic contact angles were measured with a contact angle goniometer OCA 20 (DataPhysics Instruments, Germany) equipped with SCA 20 and 21 softwares. 10 μL water drops were deposited on tested surfaces and dynamic changes of the drop profiles were recorded on 5 μL advancing and receding volumes. The profiles were fitted with the tangent leaning method. Reported values are averages of at least three measurements recorded at different positions on each substrate.

RESULTS AND DISCUSSION

Ellipsometry and Contact Angle Measurements. The measured ellipsometric thickness, the calculated PEO chain density and distance between grafting sites, the percentage of swelling when exposed to water of the different polymer layers, as well as the measured water dynamic contact angles are summarized in Table 1. The increase in PEO layer thickness corresponds very well to the increase in PEO chain length, i.e., molecular weight. With increasing PEO molecular weight (from 2000 to 20000), an increase in PEO layer thicknesses from 2.5 to 14 nm is detected which, in turn, leads to a gradual decrease in PEO chain density and an increase in distance between neighboring PEO chains. Except for the layers of PEO M_n = 20000, almost the same thicknesses were achieved for thiol layers anchored to bare gold, and thiol- and amino-PEO layers bound to PDA-modified gold

substrates. The higher thickness of PEO M_n = 20000 layers formed on PDA compared to those prepared on bare gold most probably arises from the higher amount of covalently bound PEO. A possible entanglement of non-bonded PEO M_n = 20000 chains to the covalently bonded one is excluded since it would lead to higher disorder in the layers, which was not observed in the IRRAS spectra of these layers (see below).

The water contact angles verified the anchoring of PEO chains to gold and PDA-modified gold surfaces. All layers exhibited substantial hydrophilicity with water contact angles below 30°. The contact angle values dropped with increasing thickness of the layers, i.e., increasing M_n of the polymers. Irrespective of the binding approach, the PEO layers exhibited rather similar swelling behavior with the percentage of swelling ranging from 200 to 280%.

Blood Plasma and Plasma Proteins Adsorption on PEO-Modified Surfaces

Plasma proteins (HSA, Fbg, Lys) and mixed human blood plasma (HBP) adsorption on the PEO-modified surfaces was determined using SPR. Plasma proteins were selected due to their abundance and function (e.g., stabilization of extracellular fluid volume, wound healing, clot formation, and platelet adhesion).[43–45] Furthermore, they span a wide range of sizes and weights, going from 14 kDa for Lys (40 × 30 × 30 Å) to 67 kDa for HSA (spherical shape, 72 Å), and 340 kDa for Fbg (450×90×90 Å).[29] The isoelectric points of HSA, Fbg and Lys are 4.7, 5.5 and 11.4, respectively, which means that at physiological pH, the first two proteins are negatively charged, whereas Lys carries a positive net charge.[7] Protein adsorption studies using complex biological media, e.g. HBP and/or serum, are more representative for predicting the behavior of surfaces of blood-containing devices and implanted materials.[13,30,46]

The control experiments on bare gold surfaces used in this study revealed accumulation of 93 ± 13, 265 ± 46, 112 ± 18, and 293 ± 70 ng/cm^2 of adsorbed HSA, Fbg, Lys and HBP, respectively. The fouling on bare PDA surfaces gave a level of adsorbed protein mass comparable to that of bare gold (120 ± 28, 292 ± 58, 112 ± 27, and 331 ± 38 ng/cm^2 for HSA, Fbg, Lys and HBP, respectively). The PEO layers of same molecular weight, but bound through different anchoring approaches, are characterized by almost the same thickness (and accordingly, same σ, D, and $D/2R_g$) and water contact angles (Table 1). When immersed in water all the PEO layers show similar swelling behavior as determined by *in situ* SE, irrespective of the binding approach. A tendency of lower resistance to protein adsorption was observed for the PEO-S-Au compared to the PEO layers formed on PDA.

With the exception of HSA, the adsorption trend of Fbg, Lys, and HBP on the layers formed by the PEO-S-Au approach demonstrate the increase in protein adsorption resistance with decreasing $D/2R_g$, i.e., increasing chain overlapping (Figure 1). Contrary to the PEO-S-Au layers that were prone to protein adsorption from Fbg and HSA, the PEO layers formed on the negatively charged [47] PDA reduced the protein adsorption below the detection limit of the measurement. The adsorbed mass from the positively charged Lys on the PEO layers formed on PDA was below 25 ng/cm^2. In the case of PEO-N(H)-PDA, it dropped below 1 ng/cm^2 for values of $D/2R_g < 0.24$.

Generally, the resistance to adsorption from plasma also increased with reducing $D/2R_g$, i.e., with increasing brush-like configuration of the PEO chains. The protein adsorption could be reduced to values below 30 ng/cm^2 (90% reduction compared to bare gold) in the case of PEO bound to PDA anchor layer when $D/2R_g < 0.25$, i.e., for layers of PEO with M_n = 5000. In the case of PEO(20000)-N(H)-PDA the protein adsorption from HBP was reduced to only 7 ± 2 ng/cm^2 at maximal grafting density. It is important to note that the reported values in this study are in the same range as the amounts of adsorbed proteins measured on

polymer brushes formed by surface-initiated atom-transfer radical polymerization.[30,41,48] In contrast to the substrate-independent modification approach based on PDA, the latter modification is based on rather complex reactions, difficult to control and in most cases substrate-specific.[17]

To summarize, the film thickness and contact angles indicate the presence of thick PEO films which, in contact with water, swell and form densely packed polymer brushes as predicted by the high grafting density (Table 1). Further insights into the conformation and structural order of the PEO layers in air and in water were obtained by IRRAS and VSFG spectroscopies.

IRRAS Measurements

The comparison of the IRRAS spectra in the region 950–2000 cm^{-1} of the PEO layers bound to bare gold and PDA-modified gold are shown in Figure 2. The spectra of thiol-PEO layers formed directly on gold are characterized by well-resolved narrow bands having their origin in CH_2 rocking (964 cm^{-1}), twisting (1281 and 1242 cm^{-1}), wagging (1360 and 1345 cm^{-1}), and scissoring (1467 and 1455 cm^{-1}) modes (Figure 2). The strong bands at 1120 and 1149 cm^{-1} are assigned to the C–O–C stretching mode and correspond to the polymer chain backbone in parallel and perpendicular orientations relative to the surface normal, respectively.[49,50] The narrow bands appearing in the spectra match those found in the IR spectra of well-ordered PEOs[49,50] and indicate rather uniform structure of the formed layers. The increase in M_n of the PEO caused an increase in peak intensity at 1120 cm^{-1}, but a significant decrease at 1149 cm^{-1}, indicating higher ordering of the layers with increasing M_n.[51] The presence of the peak at 1345 cm^{-1}, which becomes more prominent with increasing M_n of PEO, i.e., increasing film thickness, further proves that the EO units are in helical conformation.[50,51] All these observations confirm that, irrespective of their M_n, the PEO chains bound directly to gold surface have a brush-like structure. In the case of PEO layers anchored to PDA, the position of the characteristic PEO bands observed for those formed directly on gold remains essentially the same. The intensity decrease and the broadening of the peaks compared to the ones observed for the PEO-S-Au layers of same M_n suggest higher disorder of the polymer chains residing on PDA.

In general, the higher disorder of the PEO chains anchored to PDA caused a drop in the intensity and significant broadening of the characteristic bands originally observed for the PEO-S-Au layers. However, similarly to the layers formed by the PEO-S-Au grafting approach, the intensity of the bands at 1120 cm^{-1} and 1345 cm^{-1} increased with increasing M_n, indicating further ordering of the film, i.e., a higher number of chains in helical conformation that are perpendicularly oriented with respect to the surface normal. The highest ordering for the PEO layers formed on PDA was observed for the layers with M_n = 20000. It is noteworthy that the IRRAS data confirmed the significantly higher amount of PEO M_n = 20000 on PDA as first evidenced by SE measurements (Table 1). The larger exclusion volume usually associated with higher molecular weight polymers in good solvent is suppressed due to the melt-grafting process. This is partially responsible for the high amount of EO monomer units evident from the peak sharpness of the IRRAS spectra for M_n = 20000. Since the calculated interpenetration of the PEO chains in PDA is minimal (see Supporting Information), a factor leading to thicker PEO films of M_n = 20000 could be the higher roughness of the PDA films which would potentially provide a higher number of available grafting sites. A possible entanglement of non-covalently bound to covalently bound PEO chains (M_n = 20000) to the PDA surface is not supported by the IRRAS data (Figure 2D), since this effect would lead to higher disorder in the films.

To summarize, the data obtained by IRRAS confirmed the similar amount of PEO chains residing on gold as well as on the PDA anchor layer. For all modification approaches the

PEO chains have a brush-like structure which becomes more prominent with increasing M_n of PEO used. The PEO layers formed on gold are characterized by higher order compared to the ones formed on PDA. The IRRAS data further demonstrated the significantly higher amount of PEO chains of M_n = 20000 on PDA. The well ordered brush-like structure of these layers, i.e., with perpendicularly oriented helical PEO chains, is comparable to the one obtained by the PEO-S-Au modification approach for M_n = 10000 and 20000.

VSFG Measurements

While IRRAS is highly sensitive to molecular features such as molecular species, conformational sequences, hydrogen bonding, etc., its lack of surface sensitivity results in spectra often dominated by the film bulk contribution.[52] In order to probe only the molecular properties of the polymer/air and polymer/liquid interfaces, and to obtain information about the ordering of the PEO films in water, complementary measurements have been performed with VSFG spectroscopy due to its inherent surface selectivity and sensitivity.

VSFG Analysis of PEO Layers

In VSFG studies of the air/film interface of methoxy(-OCH_3)-terminated OEG SAM's[53,54] and PEO films prepared by solvent casting [52] it has been suggested that the generated signals predominantly arise from the terminating moieties (distal ends) of the oligomeric/polymeric chains. In all cases, a random distribution of defects and microscopic inhomogeneities was observed all over the films causing the macroscopic inversion symmetry to be preserved, and thereby, forbidding the occurrence of an SFG process arising within the film. In the case of high density, well-ordered, end-tethered polymer PEO brushes, one would also expect the VSFG spectra to be dominated by the molecular species present on the surface (i.e., OCH_3 distal ends and neighboring OCH_2 groups of the backbone). However contributions arising from the substrate/polymer and polymer/polymer interfaces, as well as from the polymer film's bulk cannot be totally excluded. VSFG spectra from PEO layers of different molecular weight anchored directly to gold and to PDA-modified gold surfaces were acquired in the C–H stretching region in air and in water. Typical VSFG spectra of PEO layers with M_n = 2000, 5000, 10000 and 20000 in air and in water are presented in Figure 3.

The similarity of the VSFG spectra obtained in air for the PEO-S-Au layers and those formed on PDA implies that the major contributions to the VSFG spectra of the latter originate mainly from PEO. Namely, during the grafting from melt at 110 °C the PEO chains protrude into the anchor layer creating an interpenetration layer (see Supporting Information).[24,25] Although the interpenetration zone thickness is minute, especially for a polymerization degree of PDA higher than ~8 monomer units, it seems that its formation causes a significant reorientation of the PDA units at the interface and most probably this absence in spectral features characteristic of PDA. However, small contributions in the VSFG spectra of PEO layers formed on PDA arising from the anchor layer (2848, 2880 cm^{-1}, 2936 cm^{-1}, and 2966 cm^{-1}, see Supporting Information, Figure S3) cannot be completely excluded.

The most prominent bands in the VSFG spectra in air of PEO-S-Au layers appear at 2857 ± 5 cm^{-1} and 2945 ± 6 cm^{-1} and are similar to symmetric and asymmetric CH_2 modes of the energetically most favored 2-methoxyethanol ($HOCH_2CH_2OCH_3$) conformer, namely *t*+*g*−*g*.[55] It is interesting to note that the dominant *tgt* conformer that forms the helical arrangement of the PEO strand cannot be detected. This leads us to consider that the sum of all TDMs within longer chain segments of *tgt* conformers vanishes and so does the SFG signal (Scheme 2). Following this, the detected signal is presumably associated to *t*+*g*−*g*

conformers inducing kinks in the helical chain. In this context, vibrations characteristic of the -OCH_3 group (amount < 1.6 wt.%) at the PEO/air interface (located around 2818 cm^{-1}, 2890 cm^{-1}, and 2978 cm^{-1})[52–54] are not present in any SFG spectra shown in Figure 3. It is very likely that the detected *t*+*g*−*g* conformers cause the terminal group to be randomly oriented and as a consequence the vanishing of the VSFG signal from the distal end methoxy groups.

The methylene peaks are appearing as peaks on the non-resonant background signal from the gold film (see Supporting Information) indicating an orientation of the contributing groups towards the substrate. As a methylene group at the end of the chain would rather result in destructive interference (in the form of a dip),[54] it can be assumed that the *t*+*g*−*g* conformers are located within the chain, therefore effectively reducing the film thickness in air.

As shown in Figure 3, the VSFG spectra of PEO layers change drastically upon immersion in water. The PEO-N(H)-PDA VSFG spectra are basically featureless indicating a random distribution of the polymer chains due to considerable water uptake and swelling. With all films having similar properties in terms of thickness, grafting density, etc. (Table 1), it can be concluded that neither the PDA, nor the bulk or upper part of the PEO chains are generating VSFG signals. Bearing this in mind, the spectral features for the PEO-S-Au and PEO-S-PDA layers are most likely associated to methylene groups in the vicinity of the sulfur atom. Accordingly, the features for the PEO-S-PDA layers for M_n > 5000 and for PEO-S-Au are similar for all films, except for PEO-S-Au M_n = 20000, which has the lowest grafting density.

The spectral features discussed above are centered at 2861 ± 3 cm^{-1}, 2923 ± 5 cm^{-1}, and 2950 ± 5 cm^{-1} and are associated to +*g*+*g*−*g* conformers.[55] Assuming that this is related to the EO unit adjacent to the sulfur atom, the constructive peak contribution for the corresponding CH_2 vibrations is indicative of groups oriented towards the substrate (see Scheme 2). One may speculate that the methylene groups are pointing away from water, also to gain energy because of van der Waals interactions with the substrate/PDA. While the thiol can react through Michael addition reaction, the amine can additionally form Schiff base products (Scheme 1B). So there is at least one product (angle) more for the amine. This could cause the higher grafting density (higher number of chains per nm^{-2}) and the higher disorder at the PEO-N(H)-PDA interface which could lead to weaker VSFG signal.

The absence of contributions for PEO-S-PDA at lower M_n but their presence in the PEO-S-Au VSFG spectra indicates that interpenetration of PEO and PDA is more pronounced for these films. This is in agreement with IRRAS data showing an overall lower order for these films. With similar properties between PEO-S-PDA and PEO-N(H)-PDA layers, it seems plausible that the interpenetration and subsequent lower IRRAS signal also holds true for the PEO-N(H)-PDA layer.

CONCLUSION

In this study, we show how to prepare dense PEO brushes on virtually any substrate by tethering PEO to PDA-modified surfaces. The same type of brushes were prepared on reference gold surfaces. The chain lengths of hetero-bifunctional PEOs were varied in the range of 45 to 500 oxyethylene units (M_n = 2000–20000). End-tethering of PEO chains was performed through amine and thiol headgroups from reactive polymer melts to minimize excluded volume effects. The thickness, chain density, and swelling of the PEO layers were determined using *in situ* and *ex situ* SE. The obtained chain densities of the end-tethered PEO ranged from 0.9 to 0.4 [chain per nm^{-2}] for M_n ranging from 2000 to 20000. The

hydrophilic character of the layers increased with increasing M_n of PEO. The level of protein adsorption of HSA and Fbg solutions was below the detection limit of the SPR measurements for all PEO layers formed on PDA exceeding the protein resistance of PEO layers tethered directly on gold. It was found that the surface resistance to adsorption of Lys and HBP increased with increasing length and brush-like character of the PEO chains end-tethered to PDA with a similar or better resistance in comparison to PEO layers on gold. The adsorption from plasma on the PEO layers formed on PDA could be reduced to less than 90% compared to the adsorbed plasma on bare gold. The brush-like structure of the polymer chains was detected for all films in air showing an increasing order with PEO M_n for the PDA-grafted films as evidenced by IRRAS. The VSFG data in air is complementary to the IRRAS data in that it probes defects in the helical conformation of the PEO chains. These are predominantly in a $t+g-g$ conformation, in which the methylene groups are pointing towards the substrate. In contrast, the distal end methoxy groups assume a random orientation. In water, the PEO chains get hydrated and randomly oriented with the exception of the groups adjacent to the sulfur atom. A majority of these groups are in a $+g+g-g$ conformation with the methylene groups pointing towards the substrate. For PDA-tethered films of lower molecular weights, it seems likely that the higher disorder detected by IRRAS for these films is evidence of an increased interpenetration of PEO and PDA.

The PDA/PEO modification route represents not only a substrate-independent approach for protein-repellent layer formation on literally any solid substrate, but also a modification approach for precise incorporation of artificial biomimetic cell adhesion ligands. The absence of strong VSFG signals for the PEO-N(H)-PDA modification will enable us to study the specific cell/artificial ligand interactions by VSFG spectroscopy. Nevertheless, our current efforts extend also on depth profiling of the PEO/PDA interpenetration zone using time-of-flight secondary ion mass spectrometry, as well as elucidating the covalent structure and organization of PDA using VSFG spectroscopy.

Supplementary Material

Refer to Web version on PubMed Central for supplementary material.

Acknowledgments

The authors thank Michael Grunze (University of Heidelberg) for support and fruitful discussions and Petr Štěpánek for the light scattering measurements. Financial support from the Helmholtz Program BioInterfaces and the Czech Science Foundation (projects: P108/11/1857 and P108/12/P624) is gratefully acknowledged. P. K. acknowledges support from NIH Grant EB-002027 to the National ESCA and Surface Analysis Center for Biomedical Problems.

References

1. Castner D, Ratner B. Biomedical surface science: Foundations to frontiers. Surf Sci. 2002; 500:28–60.
2. Hasirci, V.; Hasirci, N. Surfaces and Interfaces for Biomaterials. Vadgama, P., editor. Wood-head Publishing Limited; Cambridge, UK: 2005. p. 29-59.Chapter Control of Polymeric Material Surfaces
3. Ladd J, Boozer C, Yu QM, Chen SF, Homola J, Jiang S. DNA-directed protein immobilization on mixed self-assembled monolayers via a Streptavidin bridge. Langmuir. 2004; 20:8090–8095. [PubMed: 15350077]
4. Vaisocherova H, Yang W, Zhang Z, Cao ZQ, Cheng G, Piliarik M, Homola J, Jiang SY. Ultralow fouling and functionalizable surface chemistry based on a zwitterionic polymer enabling sensitive and specific protein detection in undiluted blood plasma. Anal Chem. 2008; 80:7894–7901. [PubMed: 18808152]

5. Harris, J. Poly(ethylene glycol) Chemistry: Biotechnical and Biomedical Applications. Plenum Press; New York: 1992.
6. Unsworth LD, Sheardown H, Brash JL. Protein resistance of surfaces prepared by sorption of end-thiolated poly(ethylene glycol) to gold: Effect of surface chain density. Langmuir. 2005; 21:1036–1041. [PubMed: 15667186]
7. Unsworth LD, Sheardown H, Brash JL. Protein-resistant poly(ethylene oxide)-grafted surfaces: Chain density-dependent multiple mechanisms of action. Langmuir. 2008; 24:1924–1929. [PubMed: 18217777]
8. Du YJ, Cornelius RM, Brash JL. Measurement of protein adsorption to gold surface by radioiodination methods: Suppression of free iodide sorption. Colloids Surf, B. 2000; 17:59–67.
9. Unsworth LD, Tun Z, Sheardown H, Brash JL. Chemisorption of thiolated poly(ethylene oxide) to gold: Surface chain densities measured by ellipsometry and neutron reflectometry. J Colloid Interface Sci. 2005; 281:112–121. [PubMed: 15567386]
10. Unsworth LD, Sheardown H, Brash JL. Polyethylene oxide surfaces of variable chain density by chemisorption of PEO-thiol on gold: Adsorption of proteins from plasma studied by radiolabelling and immunoblotting. Biomaterials. 2005; 26:5927–5933. [PubMed: 15958239]
11. Unsworth LD, Tun Z, Sheardown H, Brash JL. In situ neutron reflectometry investigation of gold-chemisorbed PEO layers of varying chain density: Relationship of layer structure to protein resistance. J Colloid Interface Sci. 2006; 296:520–526. [PubMed: 16243344]
12. Pasche S, De Paul SM, Vörös J, Spencer ND, Textor M. Poly(L-lysine)-graft-poly(ethylene glycol) assembled monolayers on niobium oxide surfaces: A quantitative study of the influence of polymer interfacial architecture on resistance to protein adsorption by ToF-SIMS and in situ OWLS. Langmuir. 2003; 19:9216–9225.
13. Tosatti S, De Paul SM, Askendal A, VandeVondele S, Hubbell JA, Tengvall P, Textor M. Peptide functionalized poly(L-lysine)-g-poly(ethylene glycol) on titanium: resistance to protein adsorption in full heparinized human blood plasma. Biomaterials. 2002; 24:4949–4958. [PubMed: 14559008]
14. Zoulalian V, Zurcher S, Tosatti S, Textor M, Monge S, Robin JJ. Self-assembly of poly(ethylene glycol)-poly(alkyl phosphonate) terpolymers on titanium oxide surfaces: Synthesis, interface characterization, investigation of nonfouling properties, and long-term stability. Langmuir. 2010; 26:74–82. [PubMed: 19691273]
15. Dalsin JL, Lin LJ, Tosatti S, Vörös J, Textor M, Messersmith PB. Protein resistance of titanium oxide surfaces modified by biologically inspired mPEG-DOPA. Langmuir. 2003; 21:640–646. [PubMed: 15641834]
16. Malisova B, Tosatti S, Textor M, Gademann K, Zurcher S. Poly(ethylene glycol) adlayers immobilized to metal oxide substrates through catechol derivatives: Influence of assembly conditions on formation and stability. Langmuir. 2010; 26:4018–4026. [PubMed: 20146501]
17. Lee H, Dellatore SM, Miller WM, Messersmith PB. Mussel-inspired surface chemistry for multifunctional coatings. Science. 2007; 318:426–430. [PubMed: 17947576]
18. d'Ischia M, Napolitano M, Pezzella A, Meredith P, Sarna A, Sarna T. Chemical and structural diversity in eumelanins: Unexplored bio-optoelectronic materials. Angew Chem–Int Edit. 2009; 48:3914–3921.
19. Pop-Georgievski O, Popelka S, Houska M, Chvostova D, Proks V, Rypáček F. Poly(ethylene oxide) layers grafted to dopamine-melanin anchoring layer: Stability and resistance to protein adsorption. Biomacromolecules. 2011; 12:3232–3242. [PubMed: 21823677]
20. Binns F, King JAG, Mishra SN, Percival A, Robson NC, Swan GA, Waggott A. Studies related to chemistry of melanins. 13. Studies on structure od dooamine-melanin. J Chem Soc C. 1970; 15:2063–2070.
21. Nicolaus, RA. Melanins. Lederer, E., editor. Herman; 1968.
22. Watt AAR, Bothma JP, Meredith P. The supramolecular structure of melanin. Soft Matter. 2009; 5:3754–3760.
23. Proks V, Jaroš J, Pop-Georgievski O, Kučka J, Popelka S, Dvořák P, Hampl A, Rypáček F. "Click & Seed" approach to the biomimetic modification of material surfaces. Macromol Biosci. 2012; 12:1232–1242. [PubMed: 22837159]

24. Zdyrko B, Klep V, Luzinov I. Synthesis and surface morphology of high-density poly(ethylene glycol) grafted layers. Langmuir. 2003; 19:10179–10187.
25. Zdyrko B, Varshney SK, Luzinov I. Effect of molecular weight on synthesis and surface morphology of high-density poly(ethylene glycol) grafted layers. Langmuir. 2004; 20:6727–6735. [PubMed: 15274578]
26. Zhu XY, Jun Y, Staarup DR, Major RC, Danielson S, Boiadjiev V, Gladfelter WL, Bunker BC, Guo A. Grafting of high-density poly(ethylene glycol) monolayers on Si(111). Langmuir. 2001; 17:7798–7803.
27. Popelka S, Machova L, Rypáček F. Adsorption of poly(ethylene oxide)-block-polylactide copolymers on polylactide as studied by ATR-FTIR spectroscopy. J Colloid Interface Sci. 2007; 308:291–299. [PubMed: 17266980]
28. Schwendel D, Dahint R, Herrwerth S, Schloerholz M, Eck W, Grunze M. Temperature dependence of the protein resistance of poly- and oligo(ethylene glycol)-terminated alkanethiolate monolayers. Langmuir. 2001; 17:5717–5720.
29. Sofia SJ, Premnath V, Merrill EW. Poly(ethylene oxide) grafted to silicon surfaces: Grafting density and protein adsorption. Macromolecules. 1998; 31:5059–5070. [PubMed: 9680446]
30. Emmenegger CR, Brynda E, Riedel T, Sedlakova Z, Houska M, Alles AB. Interaction of blood plasma with antifouling surfaces. Langmuir. 2009; 25:6328–6333. [PubMed: 19408903]
31. Azzam, RMA.; Bashara, NM. Ellipsometry and Polarized Light. Elsevier; 2003.
32. Hilfiker JN, Singh N, Tiwald T, Convey D, Smith SM, Baker JH, Tompkins HG. Survey of methods to characterize thin absorbing films with Spectroscopic Ellipsometry. Thin Solid Films. 2008; 516:7979–7989.
33. Herzinger CM, Johs B, McGahan WA, Woollam JA, Paulson W. Ellipsometric determination of optical constants for silicon and thermally grown silicon dioxide via a multi-sample, multi-wavelength, multi-angle investigation. J Appl Phys. 1998; 83:3323–3336.
34. Štěpánek P, Koňak v. Quasielastic light scattering from polymers, colloids and gels. Advances in Colloid and Interface Science. 1984; 21:195–274.
35. Filippov SK, Konak C, Kopeckova P, Starovoytova L, Spirkova M, Stepanek P. Effect of Hydrophobic Interactions on Properties and Stability of DNA-Polyelectrolyte Complexes. Langmuir. 2010; 26:4999–5006. [PubMed: 20073519]
36. Burchard, W. Laser Light Scattering in Biochemistry. Harding, SE.; Sattelle, DB.; Bloomfield, VA., editors. Royal Society of Chemistry; 1992. p. 3-22.
37. Henn G, Bucknall DG, Stamm M, Vanhoorne P, Jerome R. Chain end effects and dewetting in thin polymer films. Macromolecules. 1996; 29:4305–4313.
38. Verreault D, Kurz V, Howell C, Koelsch P. Sample cells for probing solid/liquid interfaces with broadband sum-frequency-generation spectroscopy. Rev Sci Instrum. 1997; 81:063111/1–063111/10. [PubMed: 20590229]
39. Ward RN, Davies PB, Bain CD. Orientation of Surfactants Adsorbed on a Hydrophobic Surface. J Phys Chem. 1993; 97:7141–4143.
40. Kett PJN, Casford MTL, Davies PB. Sum Frequency Generation (SFG) Vibrational Spectroscopy of Planar Phosphatidylethanolamine Hybrid Bilayer Membranes under Water. Langmuir. 2010; 26:9710–9719. [PubMed: 20394443]
41. Gao CL, Li GZ, Xue H, Yang W, Zhang FB, Jiang SY. Functionalizable and ultra-low fouling zwitterionic surfaces via adhesive mussel mimetic linkages. Biomaterials. 2010; 31:1486–1492. [PubMed: 19962753]
42. Chen SF, Zheng J, Li LY, Jiang SY. Strong resistance of phosphorylcholine self-assembled monolayers to protein adsorption: Insights into nonfouling properties of zwitterionic materials. J Am Chem Soc. 2005; 127:14473–14478. [PubMed: 16218643]
43. Grunkemeier JM, Tsai WB, McFarland CD, Horbett TA. The effect of adsorbed fibrinogen, fibronectin, von Willebrand factor and vitronectin on the procoagulant state of adherent platelets. Biomaterials. 2000; 21:2243–2252. [PubMed: 11026630]
44. Tsai WB, Grunkemeier JM, McFarland CD, Horbett TA. Platelet adhesion to polystyrene-based surfaces preadsorbed with plasmas selectively depleted in fibrinogen, fibronectin, vitronectin, or von Willebrand's factor. J Biomed Mater Res. 2002; 60:348–359. [PubMed: 11920657]

45. Wu YG, Simonovsky FI, Ratner BD, Horbett TA. The role of adsorbed fibrinogen in platelet adhesion to polyurethane surfaces: A comparison of surface hydrophobicity, protein adsorption, monoclonal antibody binding, and platelet adhesion. J Biomed Mater Res A. 2005; 74A:722–738. [PubMed: 16037938]

46. Yang W, Xue H, Li W, Zhang JL, Jiang SY. Pursuing "zero" protein adsorption of poly(carboxybetaine) from undiluted blood serum and plasma. Langmuir. 2009; 25:11911–11916. [PubMed: 19583183]

47. Ball V. Impedance spectroscopy and zeta potential titration of dopa-melanin films produced by oxidation of dopamine. Colloids Surf, A. 2010; 363:92–97.

48. Rodriguez-Emmenegger C, Kylian O, MH, Brynda E, Artemenko A, Kousal J, Alles AB, Biederman H. Substrate-Independent Approach for the Generation of Functional Protein Resistant Surfaces. Biomacromolecules. 2011; 12:1058–1066. [PubMed: 21381652]

49. Miyazawa T, Fukushima K, Ideguchi Y. Molecular Vibrations and structure of high polymers. III. Polarized infrared spectra, normal vibrations, and helical conformation of poly(ethylene glycol). J Chem Phys. 1962; 37:2764–2776.

50. Matsuura H, Fukuhara K. Vibrational spectroscopic studies pf conformation of poly(oxyethylene).II. Conformation-spectrum correlations. J Polym Sci Polym Phys. 1986; 24:1383–1400.

51. Tokumitsu S, Liebich A, Herrwerth S, Eck W, Himmelhaus M, Grunze M. Grafting of alkanethiol-terminated poly(ethylene glycol) on gold. Langmuir. 2002; 18:8862–8870.

52. Chen Z, Ward R, Tian Y, Baldelli S, Opdahl A, Shen YR, Somorjai GA. Detection of hydrophobic end groups on polymer surfaces by sum-frequency generation vibrational spectroscopy. J Am Chem Soc. 2000; 122:10615–10620.

53. Zolk M, Eisert F, Pipper J, Eck W, Buck M, Grunze M. Solvation of oligo(ethylene glycol)-terminated self-assembled monolayers studied by vibrational sum frequency spectroscopy. Langmuir. 2000; 16:5849–5852.

54. Wang RY, Himmelhaus M, Fick J, Herrwerth S, Eck W, Grunze M. Interaction of self-assembled monolayers of oligo(ethylene glycol)-terminated alkanethiols with water studied by vibrational sum-frequency generation. J Chem Phys. 2005; 122:164702/1–164702/6. [PubMed: 15945694]

55. Buck M. Ab initio calculations of vibrational spectra of 2-methoxy ethanol in the C–H stretching range. Phys Chem Chem Phys. 2003; 5:18–25.

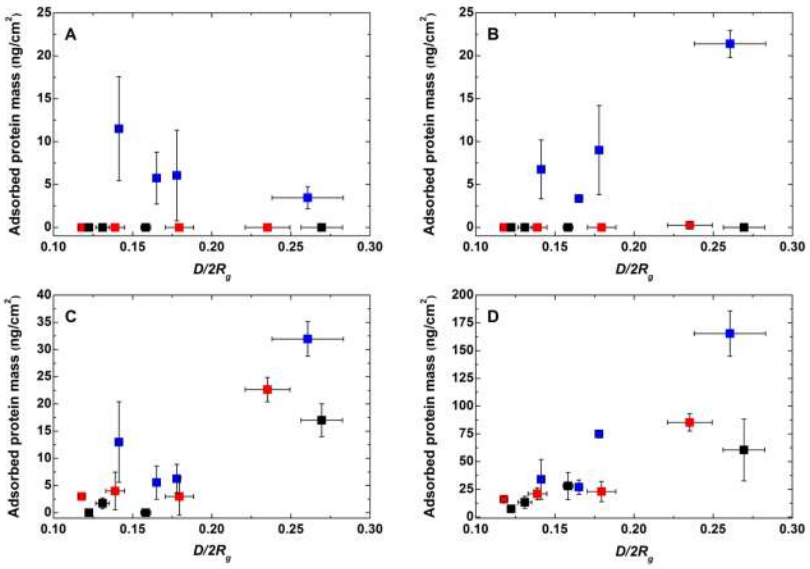

Figure 1.

Adsorbed protein mass from (A) HSA, (B) Fbg, (C) Lys, and (D) HBP versus the structure of the PEO chains. PEO-N(H)-PDA (*black*), PEO-S-PDA (*red*), and PEO-S (*blue*) anchored on gold are shown. The bare gold surfaces used in this study revealed accumulation of 93 ± 3, 265 ± 46, 112 ± 18, and 293 ± 70 ng/cm^2 of adsorbed HSA, Fbg, Lys and HBP, respectively. The fouling on PDA surfaces was on the same level of adsorbed protein mass as in the case of bare gold. The detection limit of the measurements was 0.7 ng/cm^2.

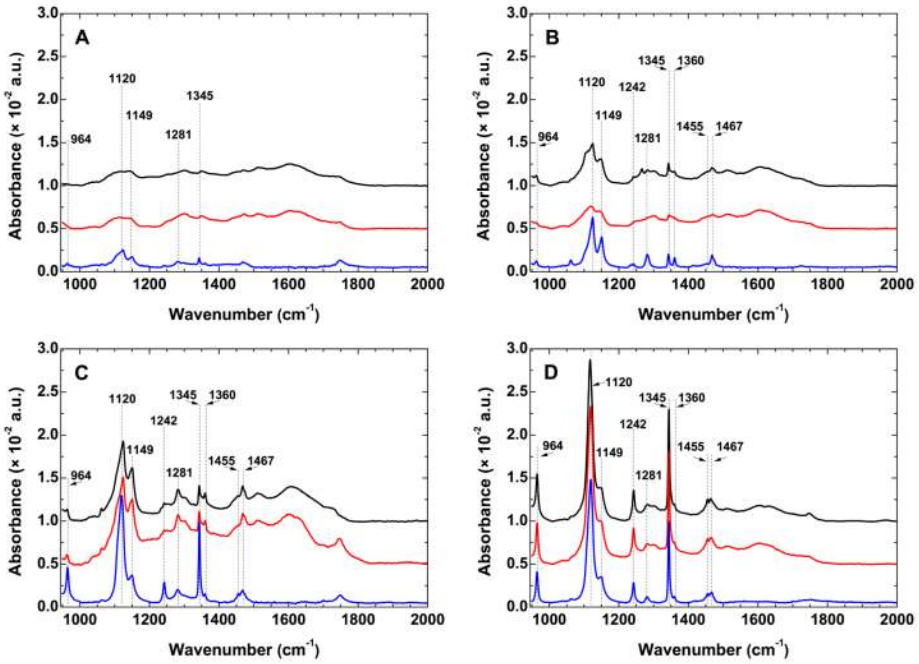

Figure 2.

IRRAS spectra in the fingerprint and amide I regions of PEO layers with different number average molecular weights: (A) 2000, (B) 5000, (C) 10000, and (D) 20000. PEO-N(H)-PDA (*black*), PEO-S-PDA (*red*), and PEO-S (*blue*) anchoring on gold are shown. Thicknesses and surface-related parameters of the layers are summarized in Table 1.

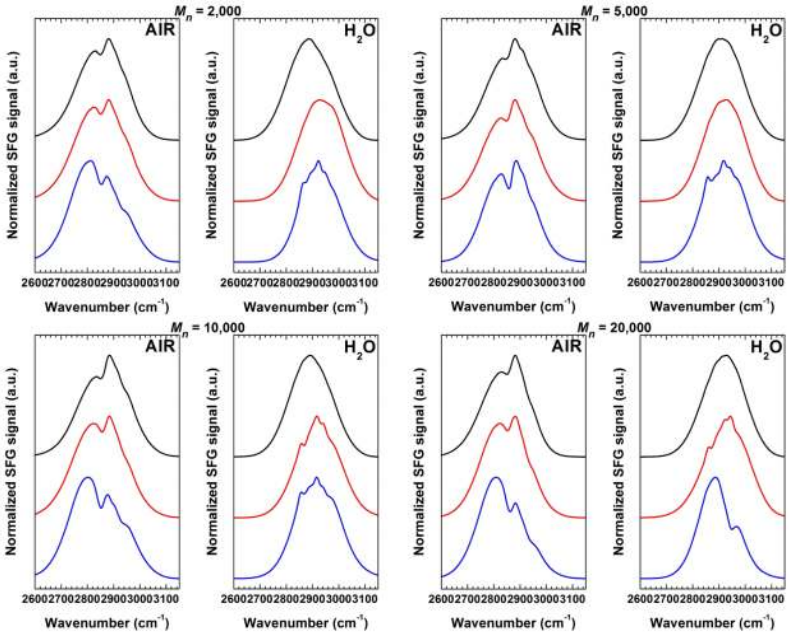

Figure 3.

VSFG spectra in the C–H region of PEO layers with different number average molecular weights: 2000, 5000, 10000 and 20000 in air and in water. Measured VSFG spectra for PEO-N(H)-PDA (*black*), PEO-S-PDA (*red*), and PEO-S (*blue*) anchoring approaches are shown.

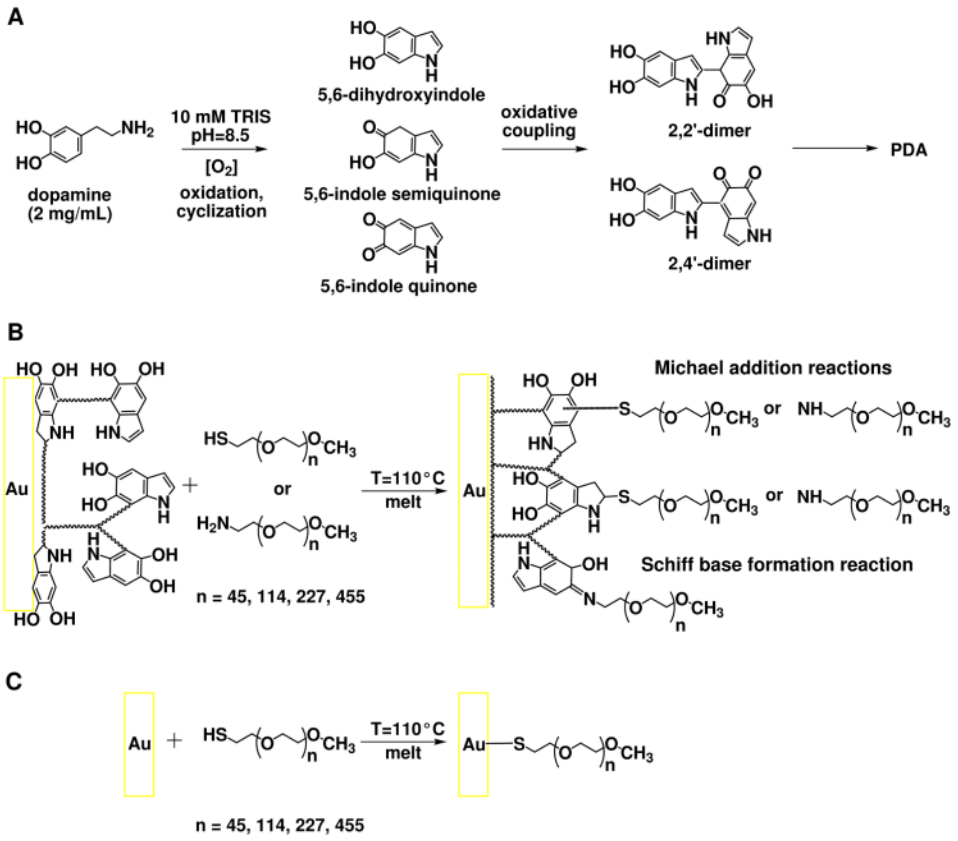

Scheme 1.

(A) Simplified mechanism of PDA formation. (B) Binding of α-thiolethyl-ω-methoxy-PEO and α-aminoethyl-ω-methoxy-PEO chains to PDA-modified Au substrates by Michael addition of nucleophilic terminus of the polymer chain on the unsaturated indole rings, and Schiff base formation reactions between the amine terminus of the polymer chain and catechols. [17] (C) Reference binding through thiolate formation between α-thiolethyl-ω-methoxy-PEO and bare Au surface.

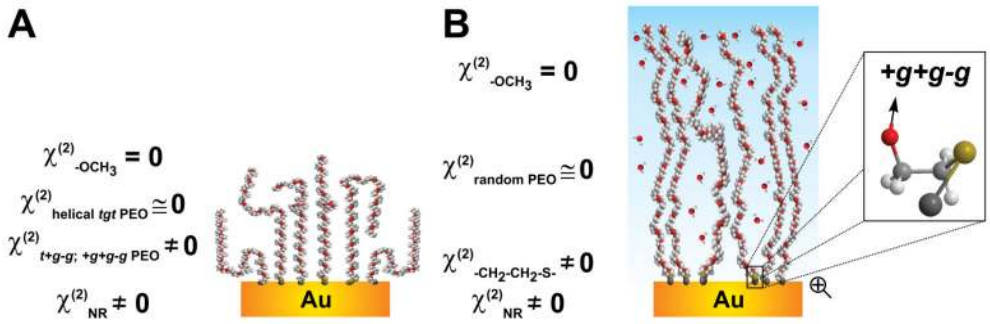

Scheme 2.

Structure of PEO brushes anchored to bare gold in (A) air and in (B) water. The CH_2 groups around the *t*+*g*−*g* conformers are preferentially oriented towards the substrate and are all pointing in one direction (see Supporting Information, and the presence of peaks in the VSFG spectra of Figs. S4 and S5), whereas the methyl groups with their random orientations do not give rise to a VSFG signal.

Table 1

Ellipsometric thickness (h) of polymer layers, PEO grafting density (σ), distance between grafting sites (D), as well as advancing (Θ_a) and receding (Θ_r) water contact angles of the bare and modified substrates. The parameter $D/2R_g$ indicates the degree of overlapping between the neighboring chains in the water environment and, in turn, the type of PEO chain structure. The percentage of swelling p_{H_2O} of different layers determined by *in situ* SE is also reported.

Layer	h [nm]		σ [nm^{-2}]	D [nm]	Θ_a [°]	Θ_r [°]	$D/2R_g$	p_{H_2O} [%]
	PDA	PEO						
Au					58±2	46±3		
PDA	11.2 ± 1.3				61±3	30±6		21
PEO(2000)-S-Au		2.5±0.5	0.8±0.15	1.3±0.1	28±1	24±1	0.26 ±0.02	270
PEO(2000)-S-PDA/Au	12.6±1.3	3.1±0.4	0.9±0.1	1.2±0.1	32±1	24±1	0.24 ±0.02	270
PEO(2000)-N(H)-PDA/Au	10.9±0.9	2.6±0.3	0.8±0.1	1.3±0.1	29±1	17±3	0.27 ±0.01	280
PEO(5000)-S-Au		5.6±0.2	0.7±0.02	1.4±0.02	16±1	12±1	0.18 ±0.002	240
PEO(5000)-S-PDA/Au	12.3±1.1	5.5±0.6	0.6±0.1	1.4±0.1	28±1	16±1	0.18 ±0.01	280
PEO(5000)-N(H)-PDA/Au	11.0±0.7	8.1±0.8	0.9±0.04	1.2±0.02	29±3	13±4	0.16 ±0.003	250
PEO(10000)-S-Au		8.6±0.2	0.5±0.01	1.7±0.02	12±1	9±1	0.14 ±0.001	220
PEO(10000)-S-PDA/Au	11.8±1.2	8.9±0.8	0.5±0.04	1.6±0.1	23±2	8±2	0.14 ±0.01	220
PEO(10000)-N(H)-PDA/Au	10.9±0.8	9.9±0.7	0.5±0.04	1.6±0.1	21±4	14±1	0.13 ±0.004	250
PEO(20000)-S-Au		8.1±0.3	0.2±0.01	2.4±0.03	13±1	8±2	0.17 ±0.002	200
PEO(20000)-S-PDA/Au	10.2±1.0	15.9 ±0.6	0.4±0.02	1.7±0.03	14±1	9±2	0.12 ±0.002	230
PEO(20000)-N(H)-PDA/Au	10.8±1.3	14.1 ±0.5	0.4±0.03	1.8±0.01	15±2	9±1	0.12 ±0.001	230